





## Origin of versatile polarization state in $\text{CuInP}_2\text{S}_6$

Xuanlin Zhang <sup>1,2</sup>, Chengcheng Xiao,<sup>3</sup> Zeying Zhang,<sup>4</sup> Luqi Dong,<sup>2</sup> Hui Pan,<sup>5</sup> Chao Cao,<sup>2</sup> Shengyuan A. Yang <sup>5</sup>,  
Su-huai Wei <sup>6</sup>, and Yunhao Lu <sup>2,1,\*</sup>

<sup>1</sup>State Key Laboratory of Silicon and Advanced Semiconductor Materials, School of Materials Science and Engineering, Zhejiang University, Hangzhou 310027, China

<sup>2</sup>School of Physics, Zhejiang University, Hangzhou 310027, China

<sup>3</sup>Departments of Materials and Physics, and the Thomas Young Centre for Theory and Simulation of Materials, Imperial College London, London SW7 2AZ, United Kingdom

<sup>4</sup>College of Mathematics and Physics, Beijing University of Chemical Technology, Beijing 100029, China

<sup>5</sup>Institute of Applied Physics and Materials Engineering, University of Macau, Macao S. A. R., China

<sup>6</sup>Beijing Computational Science Research Center, Beijing 100193, China



(Received 13 July 2023; revised 23 September 2023; accepted 27 September 2023; published 16 October 2023)

Exotic electric polarization-related phenomena have recently been reported in layered van der Waals material such as  $\text{CuInP}_2\text{S}_6$  and its derivatives, but the physical origin for such behaviors, especially the formation of quadrupole-well ferroelectric states and the anomalous polarization switching between these states, has not been clearly understood. Here, we provide a simple theoretical explanation using group theory analysis, highlighting the role of local symmetry-determined orbital interactions between copper ions and surrounding ligands. Based on this theory, we predict a surprising effect: carrier doping, which is commonly believed to suppress electric polarization, can lead to enhanced polarization in  $\text{CuInP}_2\text{S}_6$ . Our first-principles simulations confirm this unusual effect and further show that an elevated hole doping level can cause electric polarization to give way to emerging ferromagnetism. Our results not only pave a way to realize ferroelectric metals, but also broaden the scope of magnetoelectric coupling mechanisms and may help enrich the potential applications of layered ferroelectric materials in the future.

DOI: [10.1103/PhysRevB.108.L161406](https://doi.org/10.1103/PhysRevB.108.L161406)

**Introduction.** Copper (Cu) is a noble metal element with many excellent or even unique physical properties. For example, besides its relatively low resistivity compared to elements from the same group, such as iron and nickel, Cu is well known for its fast diffusion in many semiconductor materials [1,2] and its role in high-temperature superconductivity [3,4]. It has been found that the special orbital character of Cu is an important factor underlying these properties. Unlike other  $3d$  elements, Cu has  $3d$  orbitals that are relatively high in energy and they can interact with  $s$  and/or  $p$  orbitals of surrounding anions in the system [5,6].

Recently, a family of Cu-based van der Waals (vdW) layered compounds has attracted great attention. These are the Cu metal thio(seleno)-phosphates  $\text{CuXP}_2\text{Y}_6$  ( $X = \text{In, Cr, Bi}$ ;  $Y = \text{S, Se}$ ) [7–9], and the most studied representative is  $\text{CuInP}_2\text{S}_6$  (CIPS). Research on CIPS has revealed a range of exotic properties. For example, few-layer CIPS was confirmed as a rare example of two-dimensional (2D) ferroelectric material with out-of-plane polarization [10]. More interestingly, CIPS and its derivatives has been shown to have four uniaxial polarization states associated with quadrupole potential wells under different Cu displacements [11,12]. These polarization states were found to be sensitive to the interlayer distance

or external strain, which results in giant negative longitudinal piezoelectricity [13,14]. Recent studies also reported enhanced polarization behavior at the  $\text{InP}_2\text{S}_6/\text{CuInP}_2\text{S}_6$  interface [15] and an interesting ferroelectric retention effect [16] in CIPS. While these phenomena have been observed experimentally and/or predicted by first-principles calculations, we do not yet have a simple and unified theoretical understanding of the underlying mechanism behind them.

In this work, first-principles calculations with group theory analysis are employed to investigate the underlying mechanisms of Cu displacements and their correlation with the polarization states in CIPS. We show that  $s$ - $d$  coupling plays a critical role in determining the Cu displacements in CIPS. The  $s$ - $d$  coupling strength is very sensitive to local site symmetry, and its competition with  $s$ - $p$  coupling as well as lattice strain results in the quadrupole-well potential profile. Based on this understanding, we predict a remarkable effect that *moderate hole doping can enhance electric polarization in CIPS*. This is contrary to the common belief that carrier doping a ferroelectric (insulator) always suppresses its polarization. Our prediction is verified by first-principles calculations on CIPS with low doping levels ( $\sim 0.02$  hole/Cu). At relatively high doping levels ( $> 0.25$  hole/Cu), we find that the electric polarization will be turned off and give way to a spontaneous ferromagnetic state. We show that our theory offers a simple and unified understanding of various experimental results on CIPS and related systems. Our work sheds light on the

\*luyh@zju.edu.cn

mechanism underlying the rich physics of CIPS family materials and suggests new routes for controlling electric and magnetic orderings in these material platforms.

**Methods.** The first-principles calculations were performed via the Vienna *Ab initio* Simulation Package (VASP) using the generalized gradient approximation with the projected augmented wave method with a 450-eV plane-wave energy cutoff. The Perdew-Burke-Ernzerhof (PBE) function was adopted for the exchange-correlation functional [17–19]. A  $\Gamma$ -centered  $k$ -point grid of  $8 \times 4 \times 4$  was applied for sampling the Brillouin zone. The energy and force threshold for structural optimization are  $10^{-5}$  eV and  $0.01$  eV/Å. The DFT-D3 vdW correction with the Becke-Jonson damping method was considered [20]. The optimized lattice constants obtained from our DFT calculations are  $a = 6.068$  Å,  $b = 10.51$  Å,  $c = 13.51$  Å, and  $\beta = 107.34^\circ$ , which match experimental ones ( $a = 6.0956$  Å,  $b = 10.5645$  Å,  $c = 13.6230$  Å, and  $\beta = 107.101^\circ$ ) well [21], with errors less than 1.0%. The projected density of states are also calculated using by the Heyd-Scuseria-Ernzerhof (HSE06) hybrid functional to compare with PBE results [22]. The  $p$ -type carrier doping is simulated by decreasing the number of electrons, and a uniform background with opposite charge is also added to ensure neutrality.

The polarizations of undoped CIPS were calculated using the modern theory of polarization as implemented in VASP [23]. For the hole-doped CIPS, we applied the hybrid Wannier function to estimate the ill-defined polarization in metal [24]. According to modern polarization theory, the polarization was obtained by calculating the electronic  $P_{\text{electrons}}$  and ionic  $P_{\text{ions}}$  contributions, respectively.

$$P_{\text{tot}} = P_{\text{ions}} + P_{\text{electrons}} = \sum_i (q_i z_i)^{\text{ions}} + \sum_n^{\text{occ}} (q_n z_n^{\text{WC}})^{\text{WFs}}, \quad (1)$$

where  $q_i$  and  $z_i$  represent the valence charge and coordinates of ions, respectively. For doped systems, we use hybrid Wannier functions incorporated in the Z2pack code [24] to obtain the Wannier center  $z_n^{\text{WC}}$ . A Berry potential is introduced for the lattice periodic part of the Bloch functions as

$$A_n(k) = i \langle u_{nk} | \nabla_k | u_{nk} \rangle. \quad (2)$$

For a one-dimensional system, the Wannier center can be refined in terms of the Berry potential using the transformations between Wannier and Bloch representations:

$$\bar{z}_n = \frac{ia_z}{2\pi} \int_{-\frac{\pi}{a_z}}^{\frac{\pi}{a_z}} dk_z \langle u_{nk} | \delta_{kz} | u_{nk} \rangle = \frac{a_z}{2\pi} \int_{-\frac{\pi}{a_z}}^{\frac{\pi}{a_z}} dk_z A_n(k_z). \quad (3)$$

And the hybrid Wannier center can be written as

$$\begin{aligned} \bar{z}_n(k_x, k_y) &= \langle n; 0, k_x, k_y | \hat{r}_z | n; 0, k_x, k_y \rangle \\ &= \frac{ia_z}{2\pi} \int_{-\frac{\pi}{a_z}}^{\frac{\pi}{a_z}} dk_z A_n(k_x, k_y, k_z). \end{aligned} \quad (4)$$

Here, for specific  $(k_x, k_y)$  string, bands that are not fully occupied under doping are discarded for approximation (the results are shown in Supplemental Material Fig. S3 [25]).

**Symmetry-controlled  $s$ - $d$  coupling.** CIPS is a vdW layered material, with each layer formed by metal cations inserted

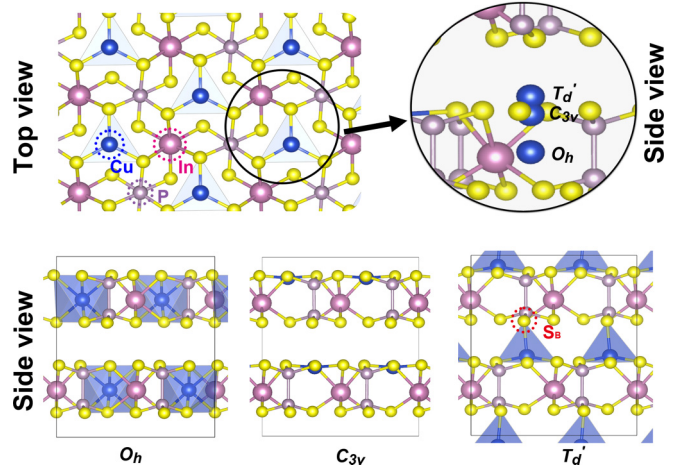


FIG. 1. The top and side view of bulk CIPS with Cu atoms at the  $O_h$ ,  $C_{3v}$ , and  $T_d'$  sites. Inset: Enlarged side view with different Cu positions.

into a hexagonal sublattice of the ethane-like  $[P_2S_6]^{4+}$  anionic unit. As shown in Fig. 1, the metal cations  $Cu^{1+}$  and  $In^{3+}$  fill the interstitial sites of this framework alternatively, forming another honeycomb sublattice. In this structure, each  $In^{3+}$  ion is relatively fixed at the position close to the center of an octahedron formed by six surrounding  $S^{2-}$  ions. Meanwhile, the position of  $Cu^{1+}$  ion may displace in the out-of-plane direction, and this displacement is the main contributor to electric polarization, as established in previous studies [21].

As illustrated in Fig. 1, we label three typical sites of the  $Cu^{1+}$  ion in the lattice depending on its out-of-plane displacement: (i) the octahedral site at the center of the  $S^{2-}$  octahedron within each layer, which has local  $O_h$  site symmetry; (ii) the triangular site at the center of the  $S^{2-}$  triangle on the side of each layer, which has a local  $C_{3v}$  symmetry; and (iii) the tetrahedral site at the center of a distorted  $S^{2-}$  tetrahedron in the vdW gap between the layers, which has an approximate  $T_d$  symmetry ( $T_d'$ ). Previous works have revealed that there is a quadrupole-well potential profile for  $Cu^{1+}$  displacement the ground state has  $Cu^{1+}$  at the triangular site, and there also exists a metastable state with  $Cu^{1+}$  located near the tetrahedral site [11, 13]. The octahedral site, on the other hand, has never been found to be stable.

To understand this quadrupole well structure, two factors have to be taken into consideration. First, the previously identified three sites have different local site symmetries. Second, the  $Cu^{1+}$  ion, with the electronic configuration of  $[Ar]3d^{10}$ , has a fully occupied  $d$  shell with energies that are close to the unoccupied  $s$  orbitals [26], which we found to be very delocalized (as shown in Supplemental Material Fig. S4 [25] and Refs. [27, 28] therein). Thus, we name these  $s$  orbitals the host  $s$  orbitals. This can be seen from the projected band structure in Fig. 2(a) obtained by first-principles calculations where Cu's  $3d$  and host  $s$  orbitals give large contributions to the bands near the Fermi level. Cu's  $3d$  orbitals mainly contribute to the states below the bandgap, and the host  $s$  orbitals mainly contribute to the state above the gap. The proximity of the orbital energies tends to enhance the  $s$ - $d$  interaction.

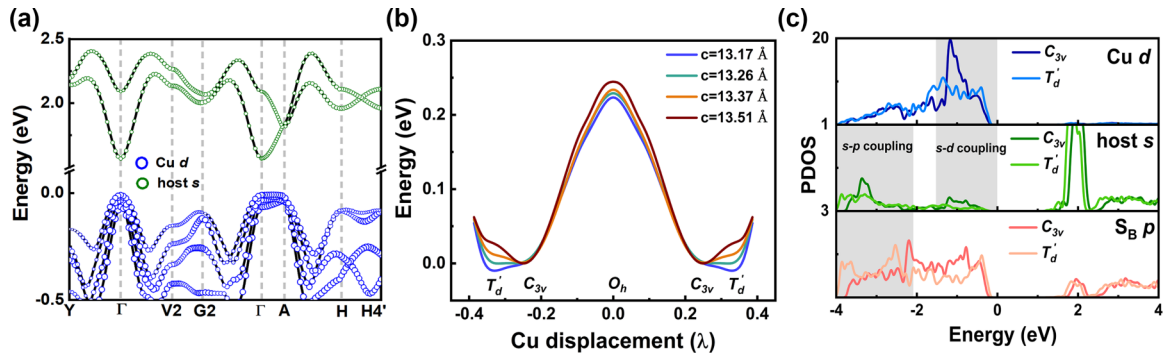


FIG. 2. (a) The projected band structure of the CIPS primitive cell with  $C_{3v}$  local symmetry. (b) Change in energy versus the Cu displacement with different  $c$  lattice;  $\lambda = 0$  and  $\lambda = 0.5$  refer to Cu in the midplane of the layer and vdW gap, respectively. The energy of the  $C_{3v}$  site is set to zero. (c) The PDOS of CIPS with Cu at the  $C_{3v}$  and  $T_d$  sites.

Previously, others [29,30] have shown that the  $s-d$  interaction strength is a critical factor influencing Cu ion diffusion in typical semiconductors such as silicon and CdS. Here, we find that the rich ferroelectric behaviors in CIPS share a similar origin.

The key point is that the  $s-d$  coupling sensitively depends on the local symmetry at the  $\text{Cu}^{1+}$  site. These sites belong to three types of symmetry. When the  $\text{Cu}^{1+}$  ion occupies the octahedral site (corresponding to the paraelectric state), its  $d$  orbitals split into  $e_g$  and  $t_{2g}$  subgroups of the local  $O_h$  symmetry group. Meanwhile, at the center of Brillouin zone  $\Gamma$ , the unoccupied  $s$  orbitals belong to the  $a_{1g}$  representation. Since there are no common representations between the  $d$  orbitals and the  $s$  orbitals, the  $s-d$  coupling is forbidden, which raises the total energy of the paraelectric state. When the  $\text{Cu}^{1+}$  ion moves to the triangular site, the local symmetry lowers to  $C_{3v}$  and the Cu  $d$  orbitals fall under the  $a_1$  and  $e$  representations. Meanwhile, the unoccupied  $s$  orbital transforms to an  $a_1$  representation. As a result, the  $s-d$  coupling is now allowed, and the energy of the system is lowered because of the common representation ( $a_1$ ). Finally, when the  $\text{Cu}^{1+}$  ion is at the (distorted) tetrahedral site, it has an approximate  $T_d$  symmetry. In this case, although  $s-d$  coupling is not forbidden, it is not as strong as the triangular site, which is discussed later. It is noted that the  $p-d$  coupling, although allowed by symmetry, has little effect on the energetics of pristine CIPS because both the  $p$  and  $d$  orbitals are fully occupied.

The previous analysis shows that the triangular site is favored by its stronger  $s-d$  coupling compared to the other two sites. In the meantime, the triangular site should have a larger strain energy cost than the other two (due to the shorter distance between Cu and sulfur); but, often in such structural distortions (as in the Jahn-Teller effect), the strain energy contribution is subdominant. To confirm our expectation, we compute the potential energy surface under Cu displacements. Namely, we plot the change in total energy of the system (using the total energy of the  $C_{3v}$  state as reference) as a function of the  $z$  displacement of  $\text{Cu}^{1+}$  ions from the midplane (set as  $\lambda = 0$ ) of a layer (i.e., the octahedral site) (Supplemental Material Calculation Details [25]). From the results in Fig. 2(b), we find that the most stable site for  $\text{Cu}^{1+}$  is indeed the triangular site. For this state, the projected density of states

(PDOS) result clearly indicates a strong hybridization among the  $s$  and  $d$  orbitals (see Fig. 2(c) and the hybrid function results in (Supplemental Material Fig. S5 [25]), consistent with our analysis. From Fig. 2(b), one also observes that the octahedral site is a local maximum due to the forbidden  $s-d$  coupling. For the (distorted) tetrahedral site, the  $s-d$  coupling is not forbidden, but the occupied Cu  $d$  levels move up in energy compared to the triangular site, indicating that  $s-d$  coupling becomes weak. Nevertheless, each  $\text{Cu}^{1+}$  ion here has one more coordinated S ( $S_B$  from the nearby layer) than the triangular site. Therefore, the occupied  $S_B-p$  states move down in energy at the tetrahedral site because of the enhanced  $s-p$  coupling by the reduced distance between  $S_B$  and  $\text{Cu}^{1+}$ . As a result, the enhanced Cu- $S_B$  bonding partly compensates for the weakened  $s-d$  coupling at the tetrahedral site. As the interlayer space is sensitive to the out-of-plane lattice constant for vdW materials, this tetrahedral site can transform into a metastable or even the most stable site by reducing the lattice constant. This scenario is indeed confirmed by our calculation result in Fig. 2(b), which shows that the tetrahedral site becomes most stable when the lattice parameter  $c$  is less than 13.26 Å. It is noted that with a larger Cu  $z$  displacement, the tetrahedral site also has a larger electric polarization. Although the negative piezoelectric response is popular for vdW polar materials, the observed giant value of negative longitudinal piezoelectricity in CIPS results from such a shift of  $\text{Cu}^{1+}$  [11].

**Hole-doping effect.** With an understanding from the previous discussion, we can now devise another approach to transform the ground-state configuration from the triangular site (corresponding to relatively low electric polarization) to the tetrahedral site (corresponding to relatively high electric polarization). This is achieved by hole doping. The reason is that the valence band maximum (VBM) is mainly contributed by the Cu  $d$  orbitals. By depleting the  $d$  orbital occupation, we effectively lower the energy gain from the  $s-d$  coupling, which, as we have clarified, is the main factor stabilizing the triangular site configuration. Thus, we expect hole doping to change the energy difference between the triangular and tetrahedral sites. This is indeed confirmed by our calculation, as shown in Fig. 3. One can see the tetrahedral site becomes more and more stable with increasing hole-doping levels and becomes the most stable position for the Cu atoms when the



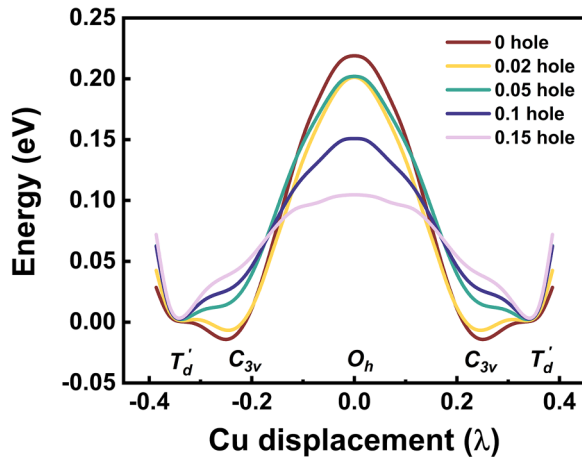


FIG. 3. Change in energy versus the Cu displacement with low doping concentration. The energy of the  $T'_d$  site is set to zero.

hole-doping concentration reaches 0.02 hole/Cu. Beyond this level, the system switches from a low electric polarization state to a high electric polarization state. This is a surprising result because, in general, carrier doping will screen the long-range dipole-dipole electrostatic interaction to suppress polar distortions [31–33]. Thus, it is difficult to realize ferroelectricity in a metallic system, although the concept of “ferroelectric metal” was raised by Anderson and Blount [34] almost 50 years ago. Only in  $\text{LiOsO}_3$  [35] and 2D  $\text{WTe}_2$  systems [36,37] has this behavior been confirmed experimentally. Carrier doping ferroelectrics [38] and superlattice design [39,40] have been proposed to enrich the ferroelectric metal families in the past ten years. The polarizations in ferroelectrics may sustain within certain carrier doping concentrations due to the “meta-screening effect” [41] or the “short-range Coulomb force” [42], but are gradually suppressed to zero with further doping. Until now, only in some special ferroelectrics where polarizations are not originated from long-range Coulomb interactions or decoupled from the electrons around the Fermi level [43–46] has carrier-induced polar distortion enhancement been predicted. Nevertheless, these phenomena are still rare and still lack experimental evidence. Here, this counterintuitive phenomenon in CIPS is enabled by a special mechanism, i.e., the doping weakens the  $s$ - $d$  coupling, changes the relative energy difference between two polarization configurations, and eventually causes the switch from a low polarization state to a high polarization state.

Our calculations show that the electric polarization of CIPS increases from  $4.26 \mu\text{C}/\text{cm}^2$  without doping to  $10.73 \mu\text{C}/\text{cm}^2$  with doping, exhibiting the anomalous enhancement of polarization by carrier doping. As in Supplemental Material Fig. S10 [25], the valence band dispersion along  $\Gamma$ -A is flat with no band crossing the Fermi level at  $T'_d$  sites, thus along the  $z$  direction the polarization can be well defined. Moreover, the corresponding conductive charge density is nonuniform and reaches zero in the vdW gap, indicating the introduced carriers may have difficulty flowing along the out-of-plane direction to screen the polar distortions completely, and the doped CIPS can be considered as a ferroelectric metal.

With a higher concentration of hole doping, the importance of  $s$ - $d$  coupling will further diminish, and crystal field splitting of the  $d$  orbitals becomes more important (see schema in Supplemental Material Fig. S7 [25]). Above 0.25 hole/Cu doping, the ground state of CIPS returns to the paraelectric state (i.e.,  $\text{Cu}^{1+}$  occupies the octahedral site). Interestingly, entering the paraelectric phase is accompanied by the emergence of a spontaneous ferromagnetic state. This magnetic ordering can be attributed to the large density of states (DOS) at the VBM around the doping level of 0.25 hole/Cu, as in Fig. 4(a) and in Supplemental Material Figs. S8 and S9 [25]. In this case, the VBM is mainly contributed by  $\text{Cu } e_g$  orbitals, giving a high DOS peak [25]. This leads to a Stoner-type ferromagnetism of  $1 \mu_B/\text{hole}$  [47,48]. The ferromagnetism is stable (20 meV/Cu lower than the antiferromagnetic configuration when doping is 0.25 hole/Cu, as shown in Supplemental Material Fig. S9(b) [25]) and is strongly coupled with the electric polarization state [Fig. 4(b)]. Thus, by controlled hole doping, we can achieve a new type of magnetoelectric coupling in CIPS.

*Discussion.* We have clarified the importance of  $s$ - $d$  coupling in CIPS, which offers a simple and unified understanding of many of its unusual behaviors. To support this picture further, we perform a comparative study of systems with Cu replaced by other elements with similar ionic radius, including Li (without  $d$  electrons), and Ni and Co (with  $d^9$  and  $d^8$  configurations, respectively). As shown in Fig. 4(c), different from CIPS, the most stable site is the paraelectric octahedral site for Li and Co, and the tetrahedral site for Ni (with similar energy to the octahedral site). Most importantly, for all these cases, the triangular site corresponds to a local maximum. The comparison highlights the special character of  $\text{Cu}^{1+}$ , which possess stronger  $s$ - $d$  couplings, and explains the nonpolar structure of metal thio(seleno)-phosphates without  $\text{Cu}^{1+}$  (e.g.,  $\text{Mn}_2\text{P}_2\text{S}_6$  and  $\text{Ni}_2\text{P}_2\text{S}_6$  [49]).

We have shown that after hole doping, CIPS can become a polar metal, even with a transition to a high polarization state at a certain doping level. From the calculated band structure in Supplemental Material Fig. S10 [25], we see that the doped system has a quasi-2D electronic character (i.e., with much less dispersion along the  $z$  direction). This suggests that external electric fields along the  $z$  direction may not be fully screened, and polarization switching could potentially be achieved just like the previous examples in  $\text{WTe}_2$  [36] and  $\text{Bi}_5\text{Ti}_5\text{O}_{17}$  [50]. Such a possibility could be explored experimentally.

The  $s$ - $d$  coupling in CIPS is sensitive to hole doping and is important for the ferroelectric transition barrier or the relative energy of different sites, which can explain the anomalous polarization switching process observed in experiments. As shown in Fig. 4(b), the transition barrier of polarization reversal can be reduced from 0.23 eV without doping to as low as 0.06 eV at a doping concentration of 0.25 hole/Cu. The vacancy of Cu ( $V_{\text{Cu}}$ ) is easy to form in CIPS due to the  $p$ - $d$  antibonding nature of the top valence band state, and holes are introduced naturally in the region around  $V_{\text{Cu}}$ . Thus, the transition barrier around  $V_{\text{Cu}}$  is much lower than the region without  $V_{\text{Cu}}$  and it is easy to flip the polarization direction around  $V_{\text{Cu}}$ . The region with few or no  $V_{\text{Cu}}$  acts as a pinning field, restraining the polarization reversal at low temperatures, which can be only activated at high temperatures. The large transition

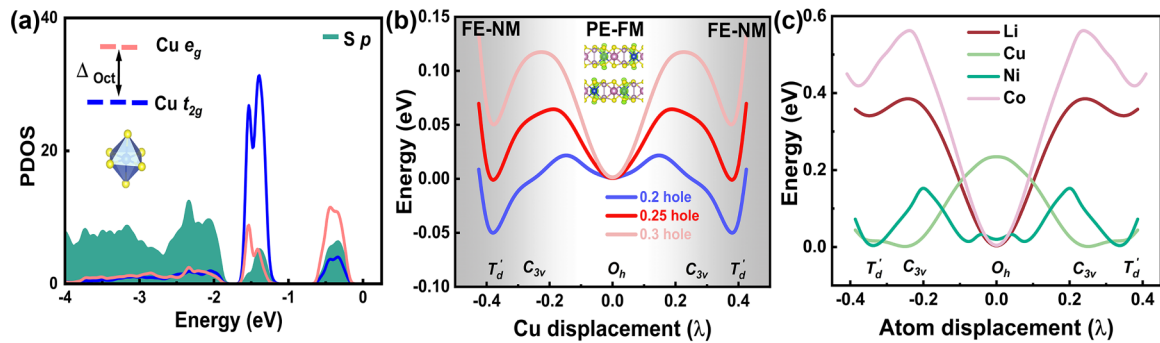


FIG. 4. (a) The PDOS of CIPS with  $O_h$  local symmetry. (b) Energy versus Cu displacement at high doping concentration. Inset: Spin density of paraelectric CIPS with 0.25 hole/Cu (isosurface 0.0015 e/Bohr<sup>3</sup>). The energy of  $O_h$  site is set to zero. (c) Energy versus monovalent ion displacement. The energy of most stable sites is set to zero.

barrier of perfect CIPS also helps to prevent the polarization reversal against fluctuation, resulting in the nearly permanent retention of polarization observed experimentally [16].

**Conclusion.** We studied the origin of the polarization state of vdW layered material CIPS by group theory analysis and first-principles calculations. The versatile polarization state in CIPS can be explained by the balance between symmetry-controlled  $s$ - $d$  and  $s$ - $p$  coupling, and the crystal field effect. The out-of-plane ferroelectricity is not suppressed, but is strongly enhanced at moderate hole doping, and ferroelectric metal can be realized in CIPS. Moreover, under high hole-doping concentrations, the paraelectric phase becomes

stable and ferromagnetism emerges due to localization of the Cu  $d$  orbitals that can be turned on and off electrically by switchable paraelectric and ferroelectric states. Therefore, our results not only pave a way to realizing ferroelectric metal, they also broaden the scope of magnetoelectric coupling mechanisms.

**Acknowledgments.** This work was financially supported by the National Key R&D Program of China (2019YFE0112000), the Zhejiang Provincial Natural Science Foundation of China (No. LR21A040001 and No. 65292, LDT23F04014F01), and the National Natural Science Foundation of China (11974307, 12274364).

- [1] H. Liu, X. Shi, F. Xu, L. Zhang, W. Zhang, L. Chen, Q. Li, C. Uher, T. Day, and G. J. Snyder, *Nat. Mater.* **11**, 422 (2012).
- [2] Z. Zhou, Y. Huang, B. Wei, Y. Yang, D. Yu, Y. Zheng, D. He, W. Zhang, M. Zou, J. Lan, J. He, C. Nan, and Y. Lin, *Nat. Commun.* **14**, 2410 (2023).
- [3] C. W. Chu, P. H. Hor, R. L. Meng, L. Gao, Z. J. Huang, and Y. Q. Wang, *Phys. Rev. Lett.* **58**, 405 (1987).
- [4] A. Schilling, M. Cantoni, J. D. Guo, and H. R. Ott, *Nature (London)* **363**, 56 (1993).
- [5] F. C. Zhang and T. M. Rice, *Phys. Rev. B* **37**, 3759 (1988).
- [6] K. Yang, H. Yang, Y. Sun, Z. Wei, J. Zhang, P.-H. Tan, J.-W. Luo, S.-S. Li, S.-H. Wei, and H.-X. Deng, *Sci. China Phys. Mech. Astron.* **66**, 277311 (2023).
- [7] M. A. Susner, M. Chyasnachyus, M. A. McGuire, P. Ganesh, and P. Maksymovych, *Adv. Mater.* **29**, 1602852 (2017).
- [8] Y. Lai, Z. Song, Y. Wan, M. Xue, C. Wang, Y. Yu, L. Dai, Z. Zhang, W. Yang, H. Du, and J. Yang, *Nanoscale* **11**, 5163 (2019).
- [9] M. A. Gave, D. Bilc, S. D. Mahanti, J. D. Breshears, and M. G. Kanatzidis, *Inorg. Chem.* **44**, 5293 (2005).
- [10] F. Liu, L. You, K. L. Seyler, X. Li, P. Yu, J. Lin, X. Wang, J. Zhou, H. Wang, H. He, S. T. Pantelides, W. Zhou, P. Sharma, X. Xu, P. M. Ajayan, J. Wang, and Z. Liu, *Nat. Commun.* **7**, 12357 (2016).
- [11] J. A. Brehm, S. M. Neumayer, L. Tao, A. O. Hara, M. Chyasnachyus, M. A. Susner, M. A. McGuire, S. V. Kalinin, S. Jesse, P. Ganesh, S. T. Pantelides, P. Maksymovych, and N. Balke, *Nat. Mater.* **19**, 43 (2020).
- [12] M. J. Swamynadhan and S. Ghosh, *Phys. Rev. Mater.* **5**, 054409 (2021).
- [13] L. You, Y. Zhang, S. Zhou, A. Chaturvedi, S. A. Morris, F. Liu, L. Chang, D. Ichinose, H. Funakubo, W. Hu, T. Wu, Z. Liu, S. Dong, and J. Wang, *Sci. Adv.* **5**, v3780 (2019).
- [14] Y. Qi and A. M. Rappe, *Phys. Rev. Lett.* **126**, 217601 (2021).
- [15] S. M. Neumayer, M. Si, J. Li, P. Liao, L. Tao, A. O. Hara, S. T. Pantelides, P. D. Ye, P. Maksymovych, and N. Balke, *ACS Appl. Mater. Inter.* **14**, 3018 (2022).
- [16] S. Zhou, L. You, A. Chaturvedi, S. A. Morris, J. S. Herrin, N. Zhang, A. Abdelsamie, Y. Hu, J. Chen, Y. Zhou, S. Dong, and J. Wang, *Mater. Horiz.* **7**, 263 (2020).
- [17] G. Kresse and J. Furthmuller, *Phys. Rev. B* **54**, 11169 (1996).
- [18] J. P. Perdew, K. Burke, and M. Ernzerhof, *Phys. Rev. Lett.* **77**, 3865 (1996).
- [19] P. E. Blochl, *Phys. Rev. B* **50**, 17953 (1994).
- [20] S. Grimme, S. Ehrlich, and L. Goerigk, *J. Comput. Chem.* **32**, 1456 (2011).
- [21] V. Maisonneuve, V. B. Cajipe, A. Simon, R. Von Der Muhll, and J. Ravez, *Phys. Rev. B* **56**, 10860 (1997).
- [22] J. Paier, M. Marsman, K. Hummer, G. Kresse, I. C. Gerber, and J. G. Ángyán, *J. Chem. Phys.* **124**, 154709 (2006).
- [23] R. D. King-Smith and D. Vanderbilt, *Phys. Rev. B* **47**, 1651 (1993).
- [24] D. Gresch, G. Autès, O. V. Yazyev, M. Troyer, D. Vanderbilt, B. A. Bernevig, and A. A. Soluyanov, *Phys. Rev. B* **95**, 075146 (2017).

- [25] See Supplemental Material at <http://link.aps.org/supplemental/10.1103/PhysRevB.108.L161406> for calculation details, host  $s$  charge density, polarization flipping barrier, schema of orbital splitting, magnetic properties, band structure, and conductive charge of doped CIPS, which includes Refs. [27,28].
- [26] S.-H. Wei, S. B. Zhang, and A. Zunger, *Phys. Rev. Lett.* **70**, 1639 (1993).
- [27] G. Henkelman, B. P. Uberuaga, and H. Jónsson, *J. Chem. Phys.* **113**, 9901 (2000).
- [28] L. Kang *et al.*, *Nat. Commun.* **11**, 3729 (2020).
- [29] J. Ma and S.-H. Wei, *Phys. Rev. Lett.* **110**, 235901 (2013).
- [30] H.-X. Deng, J.-W. Luo, S.-S. Li, and S.-H. Wei, *Phys. Rev. Lett.* **117**, 165901 (2016).
- [31] R. E. Cohen, *Nature (London)* **358**, 136 (1992).
- [32] Y. Iwazaki, T. Suzuki, Y. Mizuno, and S. Tsuneyuki, *Phys. Rev. B* **86**, 214103 (2012).
- [33] K. Uchida, S. Tsuneyuki, and T. Shimizu, *Phys. Rev. B* **68**, 174107 (2003).
- [34] P. W. Anderson and E. I. Blount, *Phys. Rev. Lett.* **14**, 217 (1965).
- [35] Y. Shi, Y. Guo, X. Wang, A. J. Princep, D. Khalyavin, P. Manuel, Y. Michiue, A. Sato, K. Tsuda, S. Yu, M. Arai, Y. Shirako, M. Akaogi, N. Wang, K. Yamaura, and A. T. Boothroyd, *Nat. Mater.* **12**, 1024 (2013).
- [36] P. Sharma, F. X. Xiang, D. F. Shao, D. Zhang, E. Y. Tsymbal, A. R. Hamilton, and J. Seidel, *Sci. Adv.* **5**, eaax5080 (2019).
- [37] Z. Fei, W. Zhao, T. A. Palomaki, B. Sun, M. K. Miller, Z. Zhao, J. Yan, X. Xu, and D. H. Cobden, *Nature (London)* **560**, 336 (2018).
- [38] T. Kolodiaznyi, M. Tachibana, H. Kawaji, J. Hwang, and E. Takayama-Muromachi, *Phys. Rev. Lett.* **104**, 147602 (2010).
- [39] S. Ghosh, A. Y. Borisevich, and S. T. Pantelides, *Phys. Rev. Lett.* **119**, 177603 (2017).
- [40] D. Puggioni, G. Giovannetti, M. Capone, and J. M. Rondinelli, *Phys. Rev. Lett.* **115**, 087202 (2015).
- [41] H. J. Zhao, A. Filippetti, C. Escorihuela-Sayalero, P. Delugas, E. Canadell, L. Bellaiche, V. Fiorentini, and J. Íñiguez, *Phys. Rev. B* **97**, 054107 (2018).
- [42] Y. Wang, X. Liu, J. D. Burton, S. S. Jaswal, and E. Y. Tsymbal, *Phys. Rev. Lett.* **109**, 247601 (2012).
- [43] S. Li and T. Birol, *Phys. Rev. Lett.* **127**, 087601 (2021).
- [44] X. He and K.-J. Jin, *Phys. Rev. B* **94**, 224107 (2016).
- [45] X. He, K.-J. Jin, H.-Z. Guo, and C. Ge, *Phys. Rev. B* **93**, 174110 (2016).
- [46] T. Shimada, T. Xu, Y. Araki, J. Wang, and T. Kitamura, *Adv. Electron. Mater.* **3**, 1700134 (2017).
- [47] E. C. Stoner, *Proc. R. Soc. London A* **165**, 372 (1938).
- [48] H. Peng, H. J. Xiang, S. H. Wei, S. S. Li, J. B. Xia, and J. Li, *Phys. Rev. Lett.* **102**, 017201 (2009).
- [49] G. Ouvrard, R. Brec, and J. Rouxel, *Mater. Res. Bull.* **20**, 1181 (1985).
- [50] A. Filippetti, V. Fiorentini, F. Ricci, P. Delugas, and J. Íñiguez, *Nat. Commun.* **7**, 11211 (2016).